Thermochimica Acta, 121 (1987) 71–86
Elsevier Science Publishers B.V., Amsterdam – Printed in The Netherlands

CHARACTERIZATION OF THE LOW-TEMPERATURE ASH COMPONENT OF THE HERRIN 6 COAL SEAM (SOUTHWESTERN ILLINOIS) BY THERMAL METHODS OF ANALYSIS *

C.M. EARNEST

Department of Chemistry, Berry College, Mount Berry Station, Rome, GA 30149 (U.S.A.)

(Received 19 December 1986; in final form 9 February 1987)

ABSTRACT

A low-temperature ash (LTA) specimen of the Herrin No. 6 Seam (Southwestern Illinois) was analyzed using the computerized thermal analysis techniques of differential thermal analysis (DTA), thermogravimetry (TG), and derivative thermogravimetry (DTG). The major features of the thermal curves were dominated by a large pyrite (FeS_2) and hydrated iron sulfate component, illite and illite–smectite mixed-layer clays, and a small calcite component. The presence of hydrated iron(II) sulfates was observed to catalyze the decomposition of pyrite in inert atmospheres. The presence of large amounts of iron oxides, generated from studies in dynamic air (oxidizing) atmospheres, was observed to interact or change the nature of the calcite decomposition relative to that normally obtained by DTA and DTG techniques.

The use of multiple atmosphere techniques allowed the recognition of pyrite in DTA as both an endothermic event in flowing nitrogen and carbon dioxide and as a multi-step exothermic event in dynamic air atmosphere. Due to the fact that ferrous sulfate heptahydrate exhibits a different mechanism for the loss of the final water of hydration in inert atmospheres than in oxidizing atmospheres, recognition of ferrous sulfate monohydrate was possible by both DTA and DTG thermal curves.

The amount of calcite present in the LTA specimen was quantified in dynamic carbon dioxide atmosphere by thermogravimetry. This value was compared to that found by X-ray diffractometry. Sulfur analysis and X-ray diffraction data were also obtained for this LTA specimen.

INTRODUCTION

The technique of low-temperature ashing of coal specimens offers a convenient method of separation of the mineral matter component(s). The procedure has been well described in the literature by Frazier and Belcher

* It is both an honor and a pleasure to make this contribution to this special issue of this journal commemorating the 60th birthday of its founder and editor. Professor W.W. Wendlandt has been one of the foremost leaders in the field of thermal analysis throughout the entire adult life of the author. His contributions as an educator, author, editor, and analytical chemist will not be matched by many. Happy Birthday Wes!

0040-6031/87/$03.50

[1] and involves the oxidation of the organic component by a low-temperature oxygen plasma. In practice, the coal is subjected to a low flow of oxygen gas which is being continuously pulsed with an RF frequency. The coal is slowly oxidized and the specimen reaches temperatures of 100–150 °C. Thus, the mineral fraction, for the most part, remains intact and is not decomposed or altered as in the high-temperature (750 °C) ashing procedures. The RF power is selected at low wattage levels for pyrite-containing coals to prevent excessive oxidation of the pyrite mineral.

The composition of the mineral matter component in the Herrin No. 6 Coal Member of the Illinois Basin has been studied extensively by Rao and Gluskoter [2]. In their study of 41 coal samples taken from different geographical locations of the Herrin 6 Seam, the overall composition of the mineral matter from this coal member was found to be: total clays (55%), pyrite (21%), quartz (15%), and calcite (9%). These results were obtained by performing X-ray diffractometry (XRD) on the low-temperature ash obtained from these specimens. The differences obtained in the analysis for the 41 samples were used to establish regional variations of the mineral components within the seam as well as to propose a model of the depositional environment for the Herrin 6 Seam.

In the study presented herein, a low-temperature ash component of a coal specimen taken from the Herrin 6 Seam in St. Clair County, Illinois, was examined by thermal methods of analysis. Preliminary XRD studies showed that this specimen was typical of that reported for the average value of the Herrin 6 Seam. The XRD estimates showed 50–55% clay mineral, 6–8% calcite, 19–22% pyrite, 2% marcasite, and 15% quartz. During the low-temperature ashing procedures, even though a low RF power of 30–40 W was employed, some pyrite was converted to iron sulfates. This low-temperature ash component was studied by differential thermal analysis (DTA), thermogravimetry (TG), and derivative thermogravimetry (DTG) in a variety of atmospheres. These descriptive thermal curves can often serve as diagnostic tools for recognition of the mineral species present as well as to describe the thermal behavior of the mineral matter in the respective atmospheres.

For the sake of brevity, in the discussion which follows, it is assumed that the reader is familiar with the thermal behavior of the clay minerals illite, kaolinite, and illite–smectite mixed-layer clays; pyrite, calcite, quartz, and the dehydration of iron(II) sulfate as observed by the techniques of DTA, TG, and DTG. Suggested background reading may be found listed in the bibliography [3–6].

EXPERIMENTAL

All DTA thermal curves reported in this work were obtained using a Perkin-Elmer microcomputer-based DTA 1700 high-temperature differential thermal analysis system. In this case, the linearized ΔT (temperature dif-

ference) signal between two Pt/Pt–10% Rh thermocouples was displayed as the ordinate signal on either a Perkin-Elmer XY_1Y_2 recorder or the Perkin-Elmer thermal analysis data station (TADS). In all cases, the linearized sample thermocouple temperature was displayed on the abscissa of the thermal curve. All TG and DTG thermal curves presented in this study were obtained with a Perkin-Elmer TGS-2 thermogravimetric analysis system used in conjunction with a System 4 microcomputer controller. Sulfur determinations were made on the LTA specimen using a Perkin-Elmer Model 240C elemental analyzer and Perkin-Elmer Model 240DS data station. The only differential scanning calorimetric experiment (Fig. 11) of this study was performed with a Perkin-Elmer DSC-2C used in conjunction with the Perkin-Elmer TADS.

The temperature axis of the DTA was calibrated using both the NBS–ICTA Quartz Reference Standard 760 and a 99.999% aluminum standard obtained from the ALFA Ventron Division of the Thiokol Corp. (Danvers, MA). The TG temperature axis was calibrated using ferromagnetic standards nickel, Perkalloy, and iron which were supplied with the instrument by the vendor.

The pyrite specimen, used either singly or in the synthetic mineral mixture studies, was obtained from the collection of Professors William R. Brice and Uldis Katkins (Department of Geology, University of Pittsburgh at Johnstown). The calcite specimen was obtained from Konrad Rieger, R.T. Vanderbilt Company, Norwalk, CT, and was originally collected in New York state.

The ferrous sulfate heptahydrate ($FeSO_4 \cdot 7H_2O$) was ACS grade (lot 092980) purchased from the Alfa Ventron Division of the Thiokol Corporation (Danvers, MA). All studies showing the use of ferrous sulfate monohydrate as a component of synthetic mineral mixtures were prepared from $FeSO_4 \cdot 7H_2O$ which had been heated to 200 °C in dynamic nitrogen in the TGS-2 thermogravimetric analysis system immediately prior to mixing with the other components of the mixture.

The low-temperature ash specimen of the Herrin 6 coal used in this study was obtained from the University of Louisville, Kentucky Energy Cabinet Laboratory, Lexington, KY. The low-temperature asher employed was an LFE Model LTA-504. An oxygen flow of 150–200 $cm^3\ min^{-1}$ was used in the asher and a low wattage RF power (30–40 W) was employed. A preliminary knowledge of the mineral composition of the ash was obtained from XRD studies performed at the Kentucky Energy Cabinet Laboratory using a Philips Model 3100 X-ray diffractometer.

RESULTS AND DISCUSSION

Figures 1, 2, and 3 give the DTA curves for the Herrin 6 Seam LTA specimen obtained in dynamic nitrogen, air, and CO_2 atmospheres, respec-

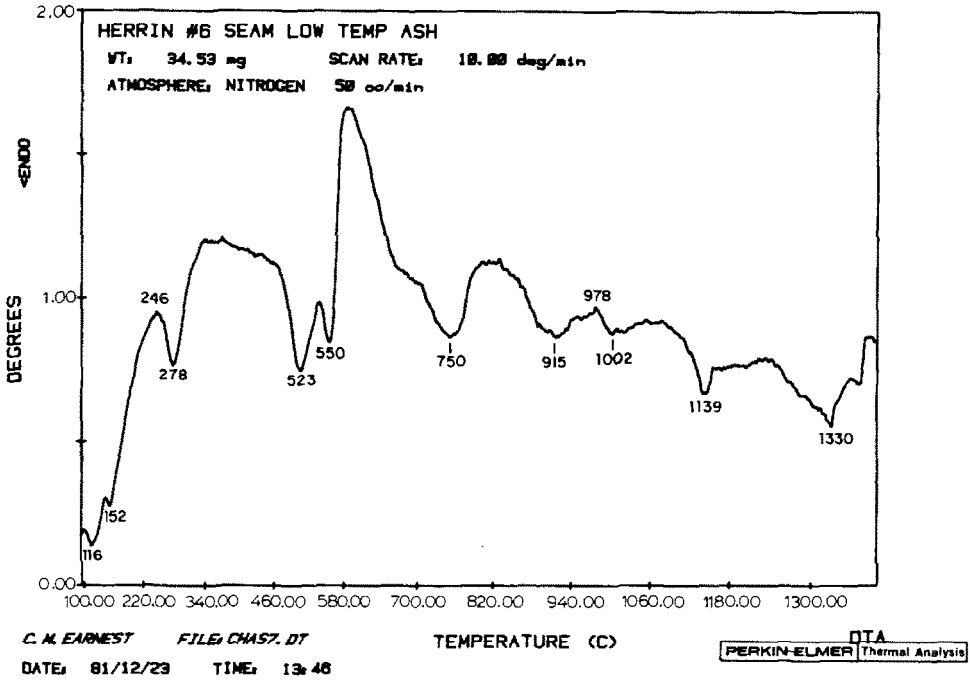

Fig. 1. DTA thermal curve for Herrin 6 LTA specimen in dynamic nitrogen atmosphere.

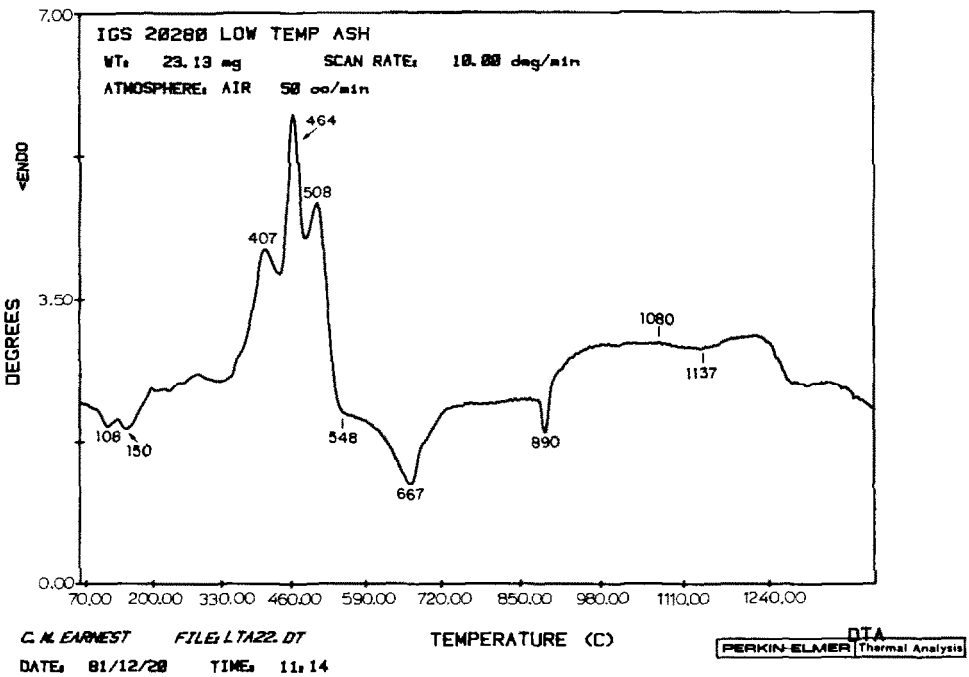

Fig. 2. DTA thermal curve for Herrin 6 LTA specimen in dynamic air atmosphere.

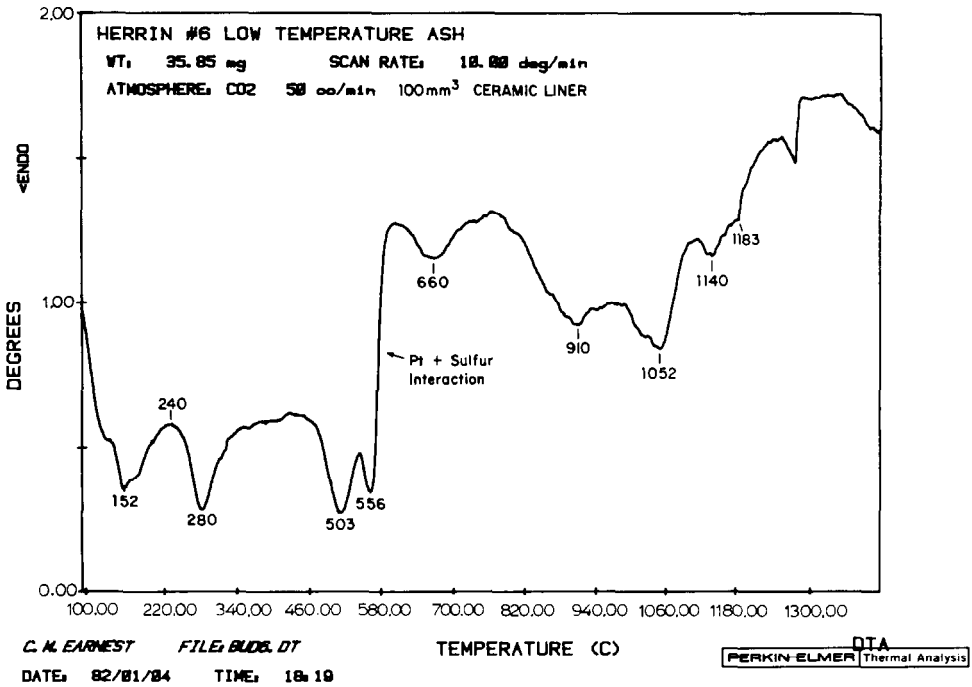

Fig. 3. DTA thermal curve for Herrin 6 LTA specimen in dynamic carbon dioxide atmosphere.

tively. The major features of these curves were dominated by a large pyrite (FeS_2) and hydrated iron sulfate component, illite and illite–smectite mixed-layer clays, and a small calcite component. The endothermic peaks observed near 110 and 150 °C in all three DTA thermal curves correspond to the loss of water from the clay mineral components as well as from the initial stages of dehydration of hydrated iron sulfate species such as $FeSO_4 \cdot 7H_2O$ (melanterite), $FeSO_4 \cdot 4H_2O$ (rozenite), and $Fe_2(SO_4)_3 \cdot 9H_2O$ (coquimbite). The endothermic peak observed at 280 °C in both dynamic nitrogen and dynamic CO_2 atmospheres corresponds to the dehydration of ferrous sulfate monohydrate (szomolnokite) to anhydrous ferrous sulfate. This peak is notably absent in the DTA curve obtained in dynamic air atmosphere. The reason for this is due to the existence of two different mechanisms for the decomposition of $FeSO_4 \cdot H_2O$ (szomolnokite) in dynamic air atmosphere. As was shown by Gallagher et al. [7], one of these routes involves the oxidation of the monohydrate to a hydroxysulfate, $Fe(OH)SO_4$, liberating water vapor. This oxidative step followed by decomposition does not produce a net endothermic effect as observed by DTA. The rippled effect observed (240–290 °C) in the DTA thermal curve given in Fig. 2, as well as the absence of the endothermic dehydration peak in this temperature region, suggests that this oxidative route to the decomposition of szomolnokite plays a major role in this case.

TABLE 1

Mechanism of $FeSO_4 \cdot 7H_2O$ decomposition (inert atmosphere or vacuum) [7]

$FeSO_4 \cdot 7H_2O \rightarrow FeSO_4 \cdot 4H_2O + 3H_2O(g)$
$FeSO_4 \cdot 4H_2O \rightarrow FeSO_4 \cdot H_2O + 3H_2O(g)$
$FeSO_4 \cdot H_2O \rightarrow FeSO_4 + H_2O(g)$
$2FeSO_4 \rightarrow Fe_2O_2SO_4 + SO_2(g)$
$Fe_2O_2SO_4 \rightarrow Fe_2O_3 + SO_3(g)$

For the convenience of the reader, Tables 1 and 2 have been included to describe the decomposition of iron(II) sulfate heptahydrate in both dynamic inert and oxidizing atmospheres. Figures 4 and 5 also provide the corresponding DTA, TG, and DTG thermal curves obtained by the author for a commercial, ACS grade, iron(II) sulfate heptahydrate specimen. These curves will assist the reader in the above discussion and throughout the remainder of this paper.

It has been observed by many that pyrite in coal matrices decomposes at lower temperatures than when heated as a single mineral specimen [8]. The same phenomenon was experienced in these studies while studying low-temperature ash materials containing known levels of pyrite. Components of the mineral matrix obviously interact with the pyrite causing either early decomposition or reaction. Since the approximate mineral content of the LTA of this study was known from XRD analysis, synthetic mineral mixtures were prepared and studied in order to first establish which components were interacting with the pyrite and, second, to observe the influence on the observed DTG or DTA thermal curve. Probably the most significant of these findings is shown in Fig. 6. The upper TG–DTG thermal curves are for the normal decomposition of pyrite to pyrrhotite in inert dynamic atmosphere for a specimen containing 23.0% FeS_2.

The lower TG–DTG thermal curves show the decomposition of the same level of pyrite in a synthetic mixture which also contains 13.76% of $FeSO_4 \cdot H_2O$. One will note, in these curves, that the dehydration of the monohy-

TABLE 2

Mechanism of $FeSO_4 \cdot 7H_2O$ decomposition (in air or oxidizing atmosphere) [7]

$FeSO_4 \cdot 7H_2O \rightarrow FeSO_4 \cdot 4H_2O + 3H_2O(g)$
$FeSO_4 \cdot 4H_2O \rightarrow FeSO_4 \cdot H_2O + 3H_2O(g)$

Two possible routes:

$2FeSO_4 \cdot H_2O + \frac{1}{2}O_2(g) \rightarrow 2Fe(OH)SO_4 + H_2O(g)$
$2Fe(OH)SO_4 \rightarrow Fe_2O(SO_4)_2 + H_2O(g)$

or

$2FeSO_4 \cdot H_2O \rightarrow 2FeSO_4 + 2H_2O(g)$
$2FeSO_4 + \frac{1}{2}O_2(g) \rightarrow Fe_2O(SO_4)_2$

$Fe_2O(SO_4)_2 \rightarrow Fe_2O_3(s) + 2SO_3(g)$

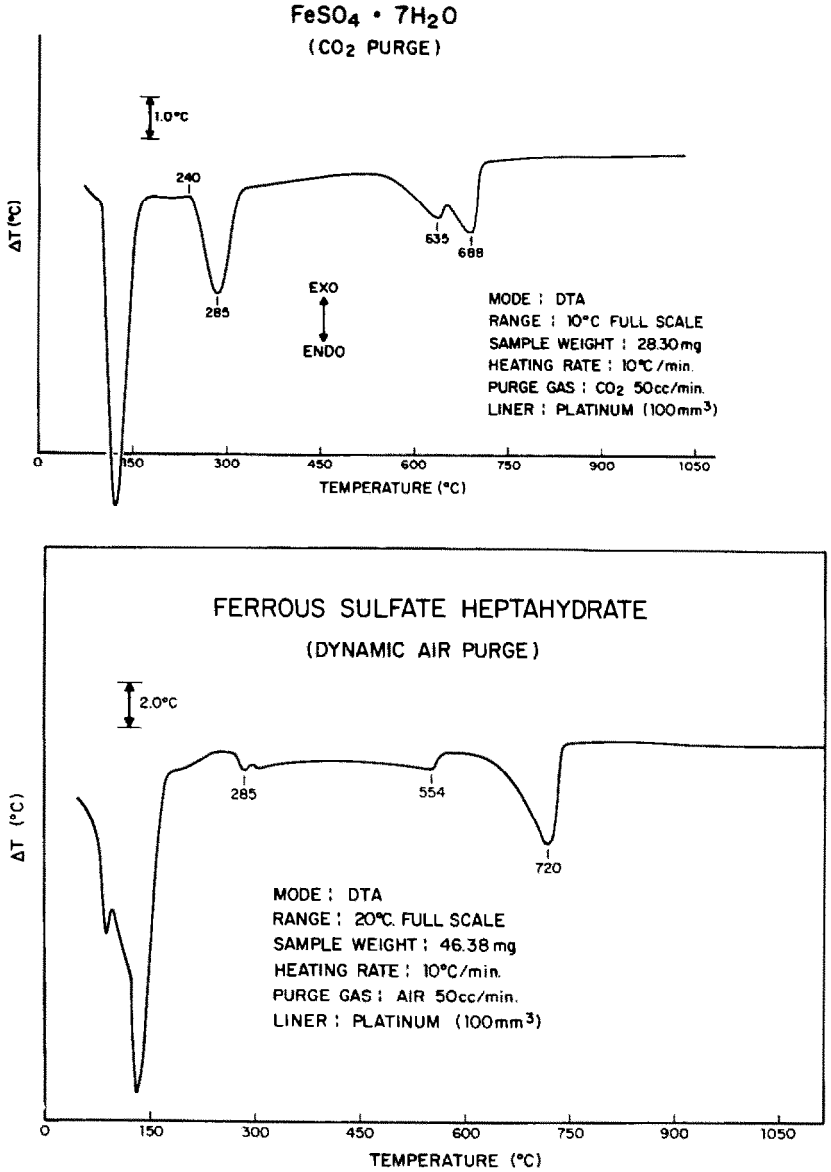

Fig. 4. DTA thermal curves for iron(II) sulfate heptahydrate in dynamic inert (upper curve) and dynamic air or oxidizing atmospheres (lower curve).

drate occurs at the usual temperature (ca. 240 °C) and at temperatures above this decomposition only anhydrous ferrous sulfate and pyrite exist in the alumina diluent matrix. A two-stage decomposition is observed with DTG maxima at 504 and 550 °C. This doublet is in good agreement with that observed in the DTA thermal curves for the Herrin 6 LTA, shown in Figs. 1 and 3, obtained in both dynamic nitrogen (T_{max} = 503 and 556 °C)

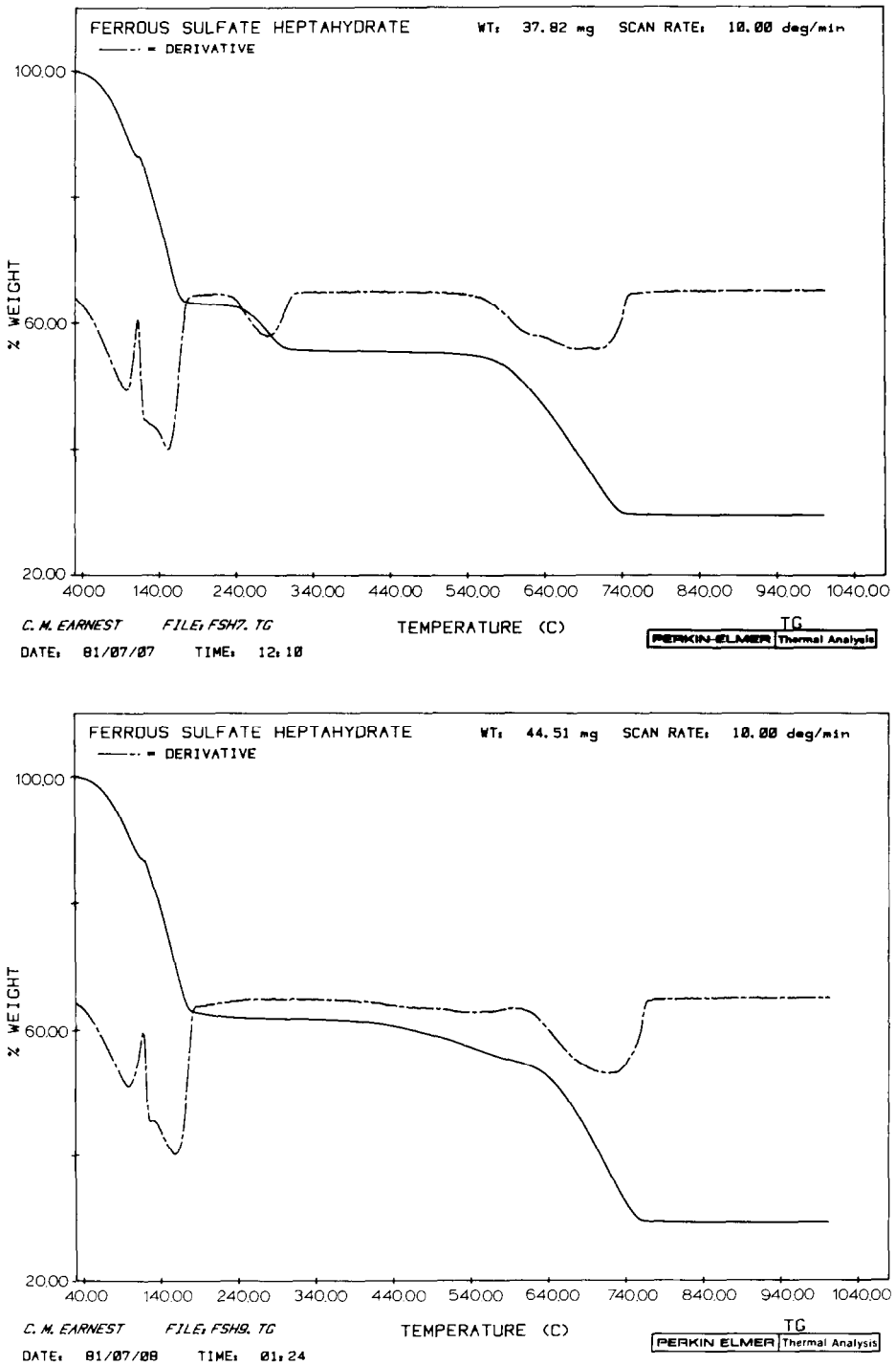

Fig. 5. TG–DTG thermal curves for iron(II) sulfate heptahydrate in dynamic inert (upper curve) and dynamic air or oxidizing atmospheres (lower curve).

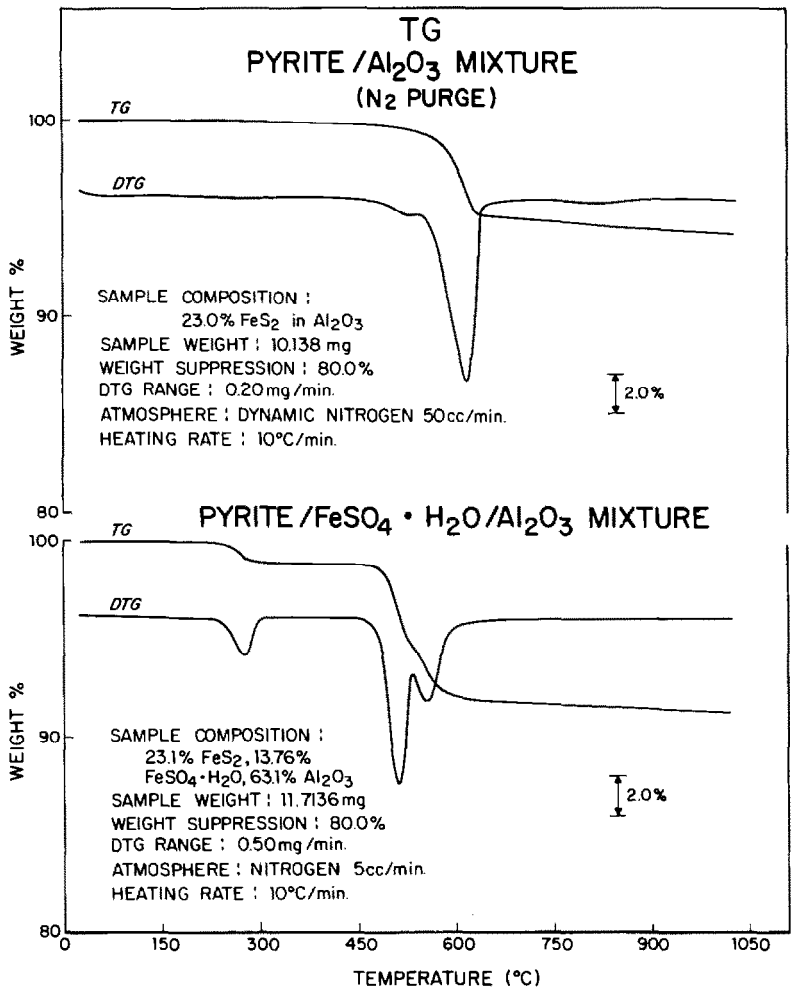

Fig. 6. TG and DTG thermal curves for pyrite (upper curves) and pyrite/iron(II) sulfate synthetic mixture (lower curves).

and dynamic CO_2 atmospheres (T_{max} = 503 and 550 °C). This doublet is not resolved in the DTG curves (Fig. 7) for the Herrin 6 Seam due to the overlap of the dehydroxylation of the clay mineral component. This overlap does not obscure the doublet in the DTA curve since the dehydroxylation for illite and illite mixed-layer clays are weakly endothermic relative to the pyrite/ferrous sulfate endothermic decomposition.

The DTA thermal curves shown in both Figs. 1 and 3 were obtained using ceramic liners in the DTA sample holder. The exothermic shift observed after the 550 and 556 °C peaks in the two curves, respectively, is due to the effect of gaseous sulfur, liberated from the decomposition of pyrite (FeS_2) to pyrrhotite ($Fe_{1-x}S$) on the platinum holder. Some interaction with the Pt/Pt–10% Rh thermocouples employed in the DTA measuring cell is also

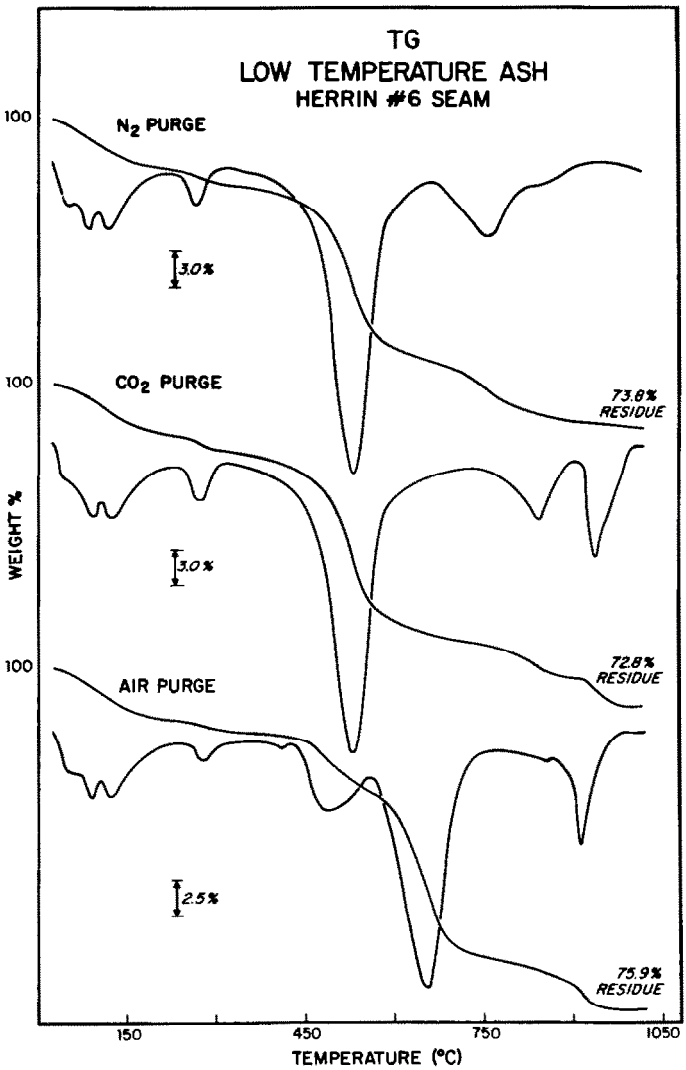

Fig. 7. TG and DTG thermal curves for Herrin 6 LTA specimen. Upper curves N_2 purge; middle, CO_2 purge; lower, dynamic air atmosphere.

possible, but these are considerably less available for attack in this DTA system than is the platinum sample holder.

This point was further verified by running another sample specimen of the LTA material using a platinum liner instead. Figure 8 shows the resulting DTA curve obtained in dynamic CO_2 atmosphere when the Herrin 6 LTA specimen was studied between 200 and 600 ° C. A potentiometric x–y recorder was used in this case for obtaining the DTA thermal curve. As one can see in Fig. 8, the orderate (ΔT) signal deflects completely off scale. The shape of the endothermic doublet is also affected by the change in liner,

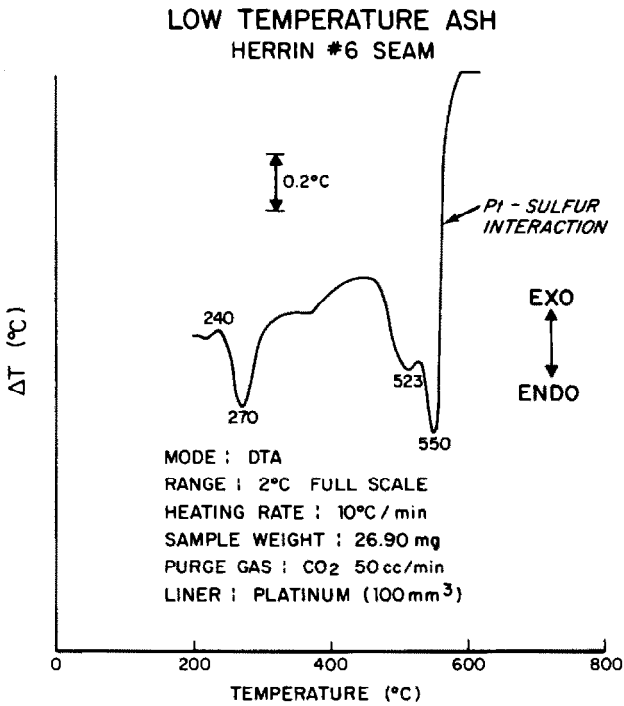

Fig. 8. DTA thermal curve for Herrin 6 LTA specimen using platinum liner in DTA sample holder.

primarily due to the shifting of the first endothermic effect to 523° C. This 20° increase in peak temperature also suggests a possible interaction with the platinum liner.

The multi-step exothermic activity observed in the DTA thermal curve in Fig. 2 at 407, 464, and 508° C corresponds to the oxidation of the large pyrite component (19% by XRD) in the presence of iron sulfates. The reader should consult a recent paper by the author for details of the multi-step pyrite oxidative peak in such LTA specimens [3]. The oxidation of the pyrite occurs at a lower temperature in such LTA specimens than that observed for the single mineral pyrite specimen. The upper TG–DTG curve in Fig. 6 can serve the reader as a reference for the oxidation of pyrite. Iron(II) sulfate is known to be an intermediate in the oxidation of pyrite to hematite (Fe_2O_3) and hence catalyzes the oxidation.

The DTA thermal curve obtained in flowing nitrogen (Fig. 1) shows an endothermic peak at 750° C which is a result of overlapping decompositions of calcite, anhydrous iron sulfate, and possibly some clay mineral matrix destruction. When the DTA curve is obtained in flowing CO_2 atmosphere, the calcite decomposition is shifted to 910° C. This can be observed in Fig. 3. The TG thermal curve obtained in dynamic nitrogen (Fig. 7, upper curve)

also shows the overlap of two weight loss events in the 700–850 °C temperature region. This corresponds to the decomposition of iron sulfates to $Fe_2O_3(s)$, $SO_2(g)$ and $SO_3(g)$ and the decomposition of calcite to CaO(s) and $CO_2(g)$. The use of dynamic CO_2 purge to separate these two weight loss events may be seen in the middle TG curve of Fig. 7. Again, the calcite decomposition is shifted to a temperature above 900 °C by the carbon dioxide atmosphere.

In the TG studies with dynamic nitrogen and CO_2 atmospheres, final decomposition of the iron sulfates in the LTA was observed at a slightly higher temperature than usual. The DTG peak for the decomposition was also broadened somewhat. This is most likely due to the effect of water vapor, generated from the previous clay mineral dehydroxylation, on the acid anhydride products of decomposition (SO_2 and SO_3) of the iron sulfate. This slight increase in peak temperature and broadening was also observed in LTA specimens from Eastern Kentucky coals containing little to no calcite or carbonate components but significant pyrite and iron sulfates in the LTA. The absence of calcite in these LTAs made it easier to observe the effect. This effect was also observed by studying a synthetic mineral mixture containing both illite–smectite mixed-layer clay minerals, kaolinite clay mineral, and 12.2% $FeSO_4 \cdot H_2O$.

When the Herrin 6 LTA specimen is studied in dynamic air atmosphere, the calcite decomposition peak undergoes a different type of separation from the other thermal events. Due to the association of the calcite component with the relatively large quantity of oxidation products of the pyrite, the calcite decomposition is both shifted to a higher peak temperature (890 °C) and sharpened. This may be observed in the DTA curve shown in Fig. 2 and in the TG and DTG curves at the bottom of Fig. 7. This observation was verified by preparing a synthetic mixture containing 7.5% calcite and 22.9% pyrite in alumina.

The TG and DTG thermal curves obtained for this synthetic mixture are given in Fig. 9 along with the TG and DTG thermal curves for the oxidation of a specimen containing 23.1% pyrite (only) in alumina. For the convenience of the reader, Fig. 10 gives the normal TG and DTG thermal curves obtained for the decomposition of calcite in dynamic air atmosphere. By comparing the slope of the leading edge of the DTG peak for the calcite decomposition in Fig. 10 with that obtained for the calcite in the pyrite/calcite/Al_2O_3 mixture of Fig. 9, one can observe the sharpening of the leading edge of the calcite decomposition peak. This peak sharpening is even more distinct in the DTA peak at 890 °C in Fig. 2. One will also note an exothermic shift of the DTA baseline immediately following this endothermic peak. This is most probably due to the combination of the free CaO(s) with $SO_3(g)$ released by the previous iron sulfate decomposition ($T_{max} = 667$ °C in Fig. 2). This is supported by an indication of weight gain in this temperature region which may be observed at the high temperatures

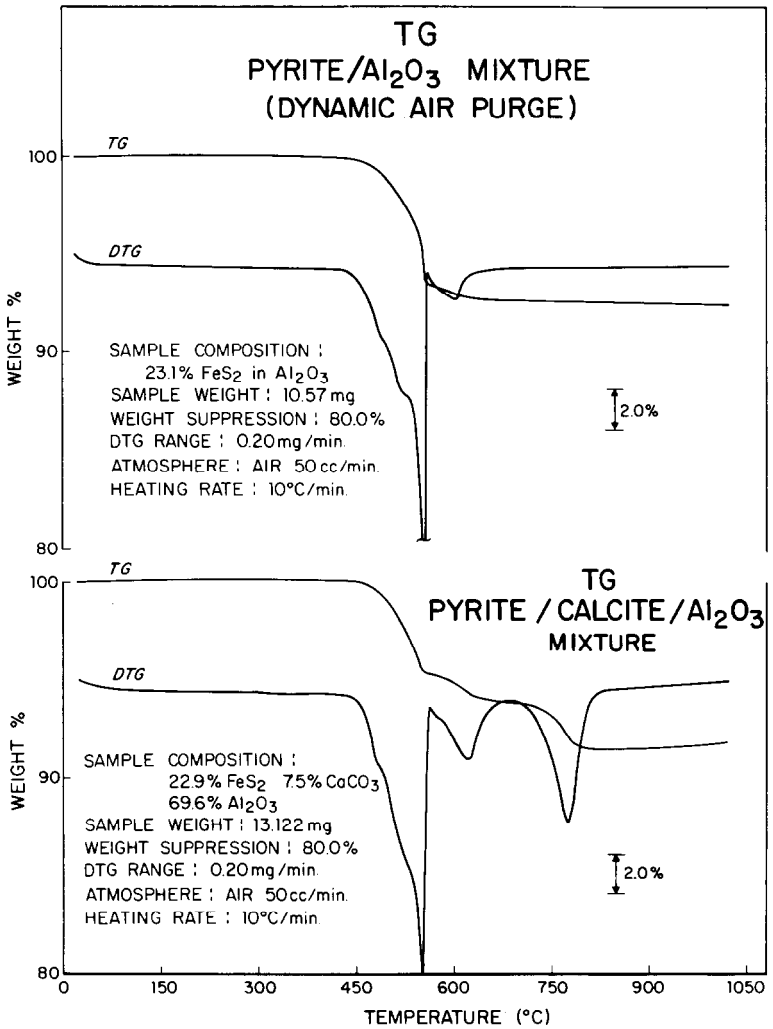

Fig. 9. TG and DTG thermal curves for pyrite/Al_2O_3 mixture (upper curves) and pyrite/calcite/Al_2O_3 mixture in dynamic air atmosphere.

of TG and DTG thermal curves for the pyrite/calcite mixture of Fig. 9 and also for the TG and DTG Herrin 6 LTA in dynamic air of Fig. 7.

The small endothermic DTA peak maxima observed at 1139°C in dynamic nitrogen (Fig. 1) and at 1140°C in dynamic CO_2 atmosphere corresponds to the melting of pyrrhotite ($Fe_{1-x}S$). This has been verified with many natural specimens in this laboratory. This endothermic event is not observed in dynamic air since the FeS_2 is oxidized to hematite and oxides of sulfur.

All other high-temperature peaks above 1000°C are left unassigned. The reader will observe the difference between the high-temperature region of

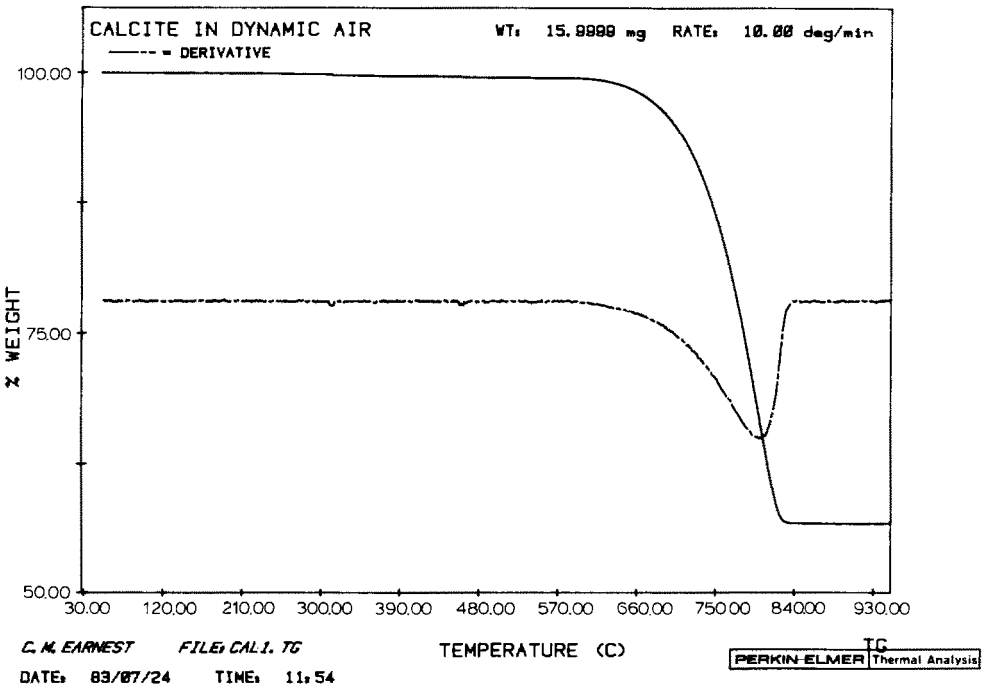

Fig. 10. TG and DTG thermal curves for decomposition of calcite in dynamic air atmosphere.

the DTA curves exhibited in dynamic nitrogen and dynamic CO_2 with that exhibited by the DTA curve obtained in dynamic air (oxidizing) atmosphere. This is primarily due to the absence of the reduced forms of sulfur and the presence of the higher oxidation state of iron.

The large clay mineral component of the Herrin 6 LTA specimen (50–55%) does play a role in influencing the behavior of the more active components calcite, pyrite, and iron sulfates. The liberation of water vapor from the dehydroxylation of the clay component provides an initially humid furnace atmosphere which is removed over a period of time. Its presence even in low concentrations can have some effect on the acid anhydride decomposition products SO_2, SO_3, and CO_2. The clay mineral dehydroxylation plays a major role in the weight loss curves and derivative weight loss curves of Fig. 7. The major TG–DTG event observed between 450 and 630 °C in both dynamic nitrogen and dynamic CO_2 atmospheres is due to the clay mineral dehydroxylation, pyrite decomposition, and weight loss due to pyrite–iron sulfate interaction. In dynamic air, this region is divided into two DTG maxima, due to the oxidation of FeS_2 and decomposition of iron sulfates.

One will note that the amount (weight %) of residue at 1025 °C is different for the three furnace atmospheres studied. The largest residue is observed in dynamic air which leads to the formation of iron(III) oxide from the pyrite component. Also, the possible formation of anhydrite, $CaSO_4$, in

this atmosphere would favor a larger residual percentage. Recent studies by Briggs and Lindsay [9] show that calcite/pyrite mixtures in coal ash heated in inert atmosphere lead to the formation of oldhamite (CaS). In their work, XRD showed that oldhamite is observed in all experiments where calcite and pyrite interact on heating in inert atmospheres and that anhydrite ($CaSO_4$) is formed only in the more oxidizing atmospheres [9].

Although the majority of the clay mineral component of the Herrin 6 LTA is composed of illite and illite–smectite mixed-layer clays, the average kaolinite content of the Herrin 6 LTA materials studied by Rao and Gluskoter [2] is 15%. Kaolinite is generally observed at this level in DTA thermal curves of LTA materials by an exothermic ordering peak between 950 and 1000 °C. The only suggestion of any kaolinite in the Herrin 6 specimen of this study is the very weakly detected exotherm at 978 °C in the DTA thermal curve of Fig. 1. Kaolinite was easily observed by DTA at levels ranging from 7 to 25% in a series of LTAs from four Eastern Kentucky coal specimens and their curves as obtained in a dynamic air purge are reported in the literature [3]. No evidence of kaolinite is seen in either dynamic air or dynamic CO_2 atmospheres by DTA of the Herrin 6 LTA specimen. Subsequent XRD studies did not find kaolinite at the expected level. This leads the author to conclude that either the specimen of

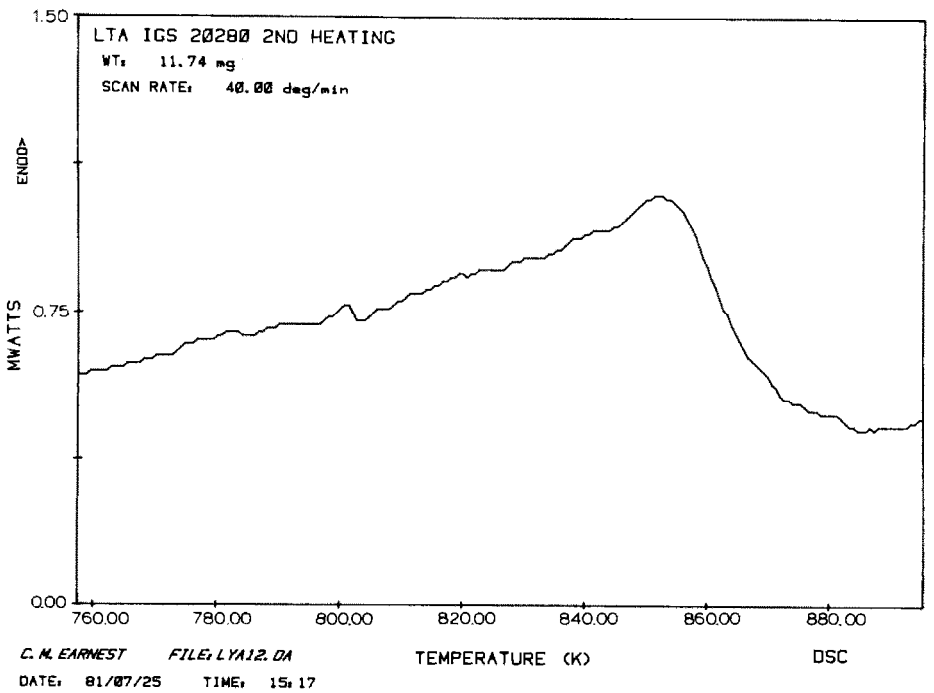

Fig. 11. DSC thermal curve for the second heating of the Herrin 6 Seam low-temperature ash.

this study contained kaolinite at a much lower level than the average Herrin 6 LTA specimen or that the kaolinite was of lower crystallinity than that generally observed by Rao and Gluskoter [2].

Due to the weak intensity of the α–β transition of quartz, which is normally observed at a peak temperature near 573° C, the quartz was not recognized in the DTA heating curve of the Herrin 6 LTA specimen. It was masked by the pyrite and clay mineral component. The quartz could be observed on second heating at elevated heating rates provided that the initial heating was not taken above 900° C. Figure 11 shows the DSC thermal curve obtained using a Perkin-Elmer power-compensated DSC-2C. This highly sensitive run is the second heating of a sample of the Herrin 6 specimen which originally weighed 11.74 mg before the initial heating to 725° C in the apparatus. The endothermic ordinate signal is an upward deflection in this instrument. The weak endothermic transition observed near 846 K (573° C) in this DSC thermal curve appears a little broader than the usual quartz transition since the temperature axis in this case is a temperature-calibrated time base.

The calcite level in the LTA was assigned from the TG weight loss curve obtained in CO_2 purge to be 5.6% as opposed to 6% assigned by XRD. The total sulfur was determined to be 9.9% of LTA using the Perkin-Elmer Model 240C elemental analyzer in the sulfur analysis mode.

ACKNOWLEDGMENTS

The author expresses his appreciation to Faith L. Fiene for the low temperature ash specimen and supporting XRD result. He also thanks Robert F. Culmo for performing the sulfur analysis of the LTA specimen.

REFERENCES

1 F.W. Frazier and C.B. Belcher, Fuel, 52 (1973) 41.
2 C.P. Rao and H.J. Gluskoter, Illinois Geological Survey Circular 476, Urbana, IL, 1973.
3 C.M. Earnest, Thermochim. Acta, 75 (1984) 219.
4 S.St.J. Warne, in Clarence Karr (Ed.), Analytical Methods for Coal and Coal Products, Academic Press, New York, 1979, pp. 447–476.
5 S.St.J. Warne, J. Inst. Fuel, 38 (1965) 207.
6 J.V. O'Gorman and P.L. Walker, Fuel, 52 (1973) 71.
7 P.K. Gallagher, D.W. Johnson and F. Schrey, J. Am. Ceram. Soc., 53 (1970) 666.
8 M. Rostam-Abadi and C.W. Kruse, Proc. 12th NATAS Conf., Williamsburgh, VA, Sept. 1983, Paper 175, 673 pp.
9 D.L. Briggs and C.G. Lindsay, ACS Div. Fuel Chem. Prepr., 29 (1984) 84.